Solar-Terrestrial Physics. 2021. Vol. 7. Iss. 2. P. 70–73. DOI: 10.12737/stp-72202107. © 2021 O.E. Yakovleva, G.P. Kushnarenko, G.M. Kuznetsova. Published by INFRA-M Academic Publishing House. Original Russian version: O.E. Yakovleva, G.P. Kushnarenko, G.M. Kuznetsova, published in Solnechno-zemnaya fizika. 2021. Vol. 7. Iss. 2. P. 77–80. DOI: 10.12737/szf-72202107. © 2021 INFRA-M Academic Publishing House (Nauchno-Izdatelskii Tsentr INFRA-M)

BEHAVIOR OF ELECTRON DENSITY IN THE IONOSPHERE OVER NORILSK DURING THE PERIOD OF DECLINING SOLAR ACTIVITY

O.E. Yakovleva
Institute of Solar-Terrestrial Physics SB RAS, Irkutsk, Russia, yakovleva@iszf.irk.ru

G.P. Kushnarenko
Institute of Solar-Terrestrial Physics SB RAS, Irkutsk, Russia, kusch@iszf.irk.ru

G.M. Kuznetsova
Institute of Solar-Terrestrial Physics SB RAS, Irkutsk, Russia, kuz@iszf.irk.ru

Abstract. We report the results of approximation of electron density N_e array obtained with a digisonde at the high-latitude station Norilsk (69.40° N, 88.10° E) during years of declining solar activity (2003–2006). The calculations are made using the author's semi-empirical model with new coefficients calculated specifically for the station Norilsk. We obtain altitudinal changes of annual variations in daily N_e at heights of the ionospheric layer F1 (120–200 km). Approximation of experimental data describes N_e quite satisfactorily at these heights. Nevertheless, there are periods with quite pronounced deviations of model values from the experiment. The presence of significant geomagnetic disturbances during these periods is probably one of the reasons for such deviations.

Keywords: electron density, annual variation, semi-empirical model (SEM).

INTRODUCTION

Geomagnetic storms are driven by the solar wind energy captured by the magnetosphere, transformed, and scattered in the high-latitude ionosphere and in the atmosphere. These periods of increased energy during disturbances cause changes in the complex morphology of electric fields, temperature, wind, and gas composition and affect all parameters of the high-latitude ionosphere. One of the main characteristics of the disturbed ionosphere is its strong variability [Buresova, Lastovicka, 2001]. There are numerous methods, including satellite, of exploration of this complex region — the high-latitude ionosphere. This paper is a sequel to articles that study the high-latitude ionosphere by our unique method [Kushnarenko et al., 2019; Yakovleva et al., 2020]. Numerous calculations carried out using the semi-empirical model (SEM) [Shepkin et al., 2008] have shown good agreement with experiments. Note that it is the general nature of the electron density N_e dependence on the gas composition and temperature of the thermosphere that enables us to apply SEM to description of the N_e behavior at 120–200 km heights under different solar and geomagnetic conditions at geographical points located at middle and partially at high latitudes.

Collecting an array of regular data on N_e with the Norilsk digisonde allowed us to approximate experimental data at F1-layer heights for a high-latitude station, using vertical sounding results and our method.

The work is based on daily hourly values of N_e at the 120–200 km height range, where in most cases during daylight hours the photochemical balance condition is met. The model calculations have been made with the coefficients obtained for given conditions of Norilsk. As a result, we obtained variations of the midday electron density in the annual cycle in the years preceding the solar minimum at fixed heights from 150 to 200 km, i.e. at the F-region heights where the F1 layer is formed under certain conditions.

We compared the electron density values calculated by SEM N_{clc} with experimental values N_{ex}. Notice that the results are valid within the frameworks of the atmospheric model NRLMSISE-00 [Picone et al., 2002] for respective neutral gas variations.

MODEL CALCULATIONS

At F1-layer heights, N_e values can be described by the analytical relation [Shepkin et al., 2008]:

$$N_e / N_{av} = X_1 + X_2 \left[n_1 / (5n_2 + n_3) \right]^{1.5} + X_3 (n_1 / n_3)^{0.5} (\cos\chi)^{0.5} + X_4 \exp\left[-(T_{ex} - 600)/600 \right] + X_5 (E / E_0). \quad (1)$$

Here, N_{av} is the average value of N_e for the entire data volume separately for each height; X_j are the coefficients of Equation (1); n_1, n_2, n_3 are concentrations of [O], [O_2], and [N_2]; T_{ex} is the exospheric temperature derived from a thermospheric model [Picone et al., 2002], χ is the solar zenith angle; E_0 is the ionizing radiation energy E at solar maximum [Tobiska, Eparvier, 1998]. To calculate the coefficients X_j of Equation (1), we have selected an array of daily hourly N_e values (7–18 LT), obtained by the Norilsk digisonde at heights of 120, 130, ..., 190, 200 km in 2003–2006. The $F10.7$, A_p, and Dst indices were taken from the database at the WDC Kyoto [http://wdc.kugi.kyoto-u.ac.jp].

These calculations yielded coefficients of approximating equation (1) for the period of declining solar activity, thereby contributing to the existing SEM ver-

sion. As an example we present coefficients for the station Norilsk (Table 1). The last column shows correlation coefficients R_{corr} between arrays of calculated and experimental N_e for the given period.

DISCUSSION

We have obtained annual variations of midday N_e at heights of 150, 180, and 200 km for a period of declining solar activity (2003–2006) at the station Norilsk. To illustrate the results, Figure plots annual electron density variations for 2003. For comparison, for each height we show experimental midday values averaged over 21 days throughout the dataset (± 10 days centered on a given day). At all the heights, there is a reasonable agreement between N_{clc} [Shchepkin, 2008] and N_{ex}.

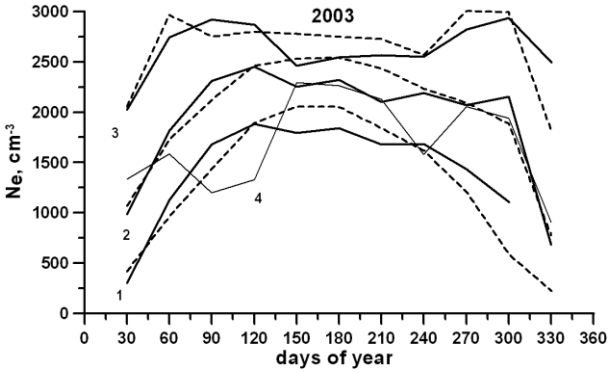

Annual variation of calculated midday electron density values N_{clc} (solid thick line) in 2003 at heights of 150 km (1), 180 km (2), and 200 km (3). Dashed lines are N_{ex} values at each height; curve (4) indicates N_e values from IRI [Bilitza et al., 2017] at a height of 200 km

Table 1

Coefficients of fitted equation (1)

h, km	N_{av},10^2 cm^{-3}	X_1	X_2	X_3	X_4	X_5	R_{corr}
120	7.51	–0.1844	–7.403	4.842	0.0000	0.9708	0.935
130	8.57	–0.4140	–7.960	5.459	0.2335	0.9473	0.904
140	10.25	–0.3128	–8.238	5.310	0.2341	0.7888	0.941
150	12.07	–0.3352	–7.917	5.106	0.4142	0.7005	0.950
160	13.80	–0.3521	–7.048	4.688	0.5798	0.7009	0.958
170	15.39	–0.3646	–5.463	4.130	0.7145	0.7496	0.960
180	17.16	–0.3462	–2.644	3.430	0.7984	0.7455	0.936
190	19.19	–0.3267	1.388	2.659	0.8516	0.7008	0.832
200	22.32	–0.3604	5.298	1.983	0.9051	0.7580	0.697

The similarity between the N_{ex} and N_{clc} curves lies in the fact that there is a summer maximum in both cases at 150 and 180 km. At high latitudes during this period, there is no phase change in the annual electron density variation at 190 and 200 km. At the height of 200 km, the annual variation in N_{clc} has unique features: there are two increases in N_{clc} on the curve during equinox periods, which is also confirmed by experiment. The curves obtained for the three heights of other years (2004–2006) differ slightly from those for 2003.

To compare with our results, we have used IRI [Bilitza et al, 2017] to calculate annual variations in midday N_e for these heights for the years under study. The N_e values from IRI are much lower than N_{ex} and our N_{clc} at all the heights of interest. In Figure, the curve obtained from IRI for 200 km is far below the curves of N_{clc} and N_{ex} for this height.

The similarity between the IRI and SEM curves is attributed to the presence of increased N_e values near equinox periods. Such a shape of IRI curves is also typical for the heights of 150 and 180 km.

CHANGE OF THE RELATION $r_1 = N_{Ex1}/N_{clc}$ IN 2003–2006

To identify deviations of N_{ex} from N_{clc}, we have found N_{clc} values for all the years under study, from which we have compiled Table 2 showing the ratios of N_{ex} to N_{clc} (r_1=N_{ex}/N_{clc}) for the height of 200 km, where diurnal and seasonal variations of N_e under different conditions are most pronounced.

Let us delve into r_1 variations during the period of interest. In 2003 and 2004, N_{ex}/N_{clc} vary around 1, showing a good fitting of the experimental array by our model. There are, however, days when N_{ex} values exceed N_{clc} by 20–35 % in 2003. We may assume that the extremely high geomagnetic activity observed in 2003 [Panasyuk et al., 2004] is likely to be the main reason for the increase in r_1. In the annual variations that occurred in 2005 and 2006, also noticeable are summer periods — from the 150th to 250th day when N_{ex} is higher than N_{clc} by 15–30 %. These days were marked by fairly significant geomagnetic disturbances with daily average A_p=27, 33, 34, 45, 47, 90. We may assume that they are somewhat responsible for the increases in r_1.

In Table 2 and Figure, we omit the electron density values at the beginning and end of the annual periods because in winter at the heights of interest the experimental electron density values are small and unreliable, which is typical for a high-latitude ionospheric station. Also worth noting is that the numerous gaps and absence of data in the tested N_e arrays at the station Norilsk in these years lead to the fact that the correlation coefficients between the arrays of calculated and experimental data on N_e for this period were obtained within 0.94–0.70, with the highest value at 120 km, and the smallest at 200 km (Table 1). The result is a difference between N_{clc} and N_{ex} at 190 and 200 km.

Table 2

$r_1 = N_{ex}/N_{clc}$, 200 km, 12 LT

Days of year	2003	2004	2005	2006
30	0.87	0.85	1.14	0.90
40	0.74	0.70	0.96	0.98
50	0.89	0.88	0.93	0.96
60	0.83	1.09	1.16	0.90
65	0.90	0.86	1.43	0.98
70	0.83	1.09	0.88	1.04
75	1.04	1.10	0.85	0.88
80	1.34	0.88	1.02	1.00
85	0.78	0.81	1.28	0.95
90	0.76	0.98	1.15	0.80
95	0.85	1.06	1.34	1.00
100	1.08	1.21	0.97	0.96
105	1.13	0.95	1.09	1.15
110	0.90	0.87	1.32	0.96
130	1.34	1.04	0.82	1.10
150	1.17	1.16	1.36	1.25
170	1.08	1.12	1.25	1.28
190	0.99	1.32	1.25	1.26
210	1.38	1.15	1.09	1.28
230	1.26	0.92	1.15	1.12
250	1.05	1.05	0.99	1.03
255	1.15	0.91	1.01	1.04
260	1.31	1.10	0.97	1.23
265	0.98	1.05	0.94	1.02
270	0.85	0.99	1.11	0.98
275	0.93	1.06	1.16	0.98
280	1.05	1.07	1.00	1.01
285	0.99	1.27	0.83	0.95
290	1.19	1.08	1.06	0.86
295	0.89	0.98	0.93	1.10
300	0.57	0.67	0.90	0.81
320	0.99	0.73	0.70	0.74

In general, we can speak of reasonable accuracy of approximation of most experimental material. Table 3 lists the calculated values N_{clc} (daytime) and experimental monthly averages N_{ex}, as well as N_{ex}/N_{clc} for April and June 2006.

The N_{ex} values exceed N_{clc} by 10–20 % in the second half of the day in April 2006 at all the heights. At another point of time, there is quite close agreement between these values.

CONCLUSION

The semi-empirical model SEM employed in the paper can describe the behavior of the ionosphere, using measurement data obtained by the vertical sounding method for the high-latitude station Norilsk. We have considered heights below 200 km during declining solar activity (2003–2006).

1. Approximation of the N_e array for these years allows us to examine the annual variation in N_e. We have found that at all heights below 200 km maximum N_e values are observed in summer; and minimum ones, in winter.

2. Comparison between arrays of experimental values N_{ex} and those calculated by SEM N_{clc} for all the years and heights considered has revealed fairly good agreement between them both in values and in shapes of annual curves.

3. Comparison between arrays of N_{ex} and electron density values derived by IRI has shown a divergence between results: IRI N_e are significantly lower at respective heights in the years under study.

4. Further collection of experimental material (digisonde) will enable us to improve the existing semi-empirical model for different heliogeophysical conditions. This model is particularly important in evaluating the thermospheric gas composition at heights of the middle ionosphere from vertical sounding data.

The work was financially supported by the Ministry of Science and Higher Education of the Russian Federation (project "Study of the state and dynamics of Earth's atmosphere at different time scales under the influence of geophysical, cosmic, and human impacts"). The results were obtained using the equipment of Shared Equipment Center «Angara» [https://ckp-rf.ru/ckp/3056].

Table 3

N_{clc}, $N_{ex}(\times 10^2)$ and N_{ex}/N_{clc} at 150, 190, and 200 km

Parameter	April 2006						June 2006					
	8 LT	10 LT	12 LT	14 LT	16 LT	18 LT	8 LT	10 LT	12 LT	14 LT	16 LT	18 LT
150 km												
N_{ex}	10.8	14.2	15.8	16.6	13.5	10.0	15.5	18.0	17.3	17.9	16.3	13.3
N_{clc}	12.3	15.1	16.1	15.2	12.5	7.40	14.3	16.3	17.2	16.8	15.0	12.2
N_{ex}/N_{clc}	0.9	0.9	1.0	1.1	1.1	1.3	1.1	1.1	1.0	1.1	1.1	1.1
190 km												
N_{ex}	18.1	20.9	23.8	27.0	25.5	17.6	20.3	22.8	22.0	23.8	22.1	20.7
N_{clc}	19.2	22.0	23.0	22.5	20.2	15.7	19.1	21.0	22.0	21.8	20.4	17.9
N_{ex}/N_{clc}	1.0	1.0	1.0	1.2	1.2	1.1	1.1	1.1	1.0	1.1	1.1	1.1
200 km												
N_{ex}	18.5	21.7	25.2	29.5	28.5	20.8	19.9	22.6	26.0	23.6	22.3	21.2
N_{clc}	21.8	24.4	25.5	25.2	23.2	19.3	20.0	21.9	22.9	22.8	21.7	19.5
N_{ex}/N_{clc}	0.9	0.9	1	1.1	1.2	1.0	1.0	1.0	1.1	1.0	1.0	1.1

REFERENCES

Bilitza D., Altadill D., Truhlik V., Shubin V., Galkin I., Reinisch B., Huang X. International Reference Ionosphere 2016: From ionospheric climate to real-time weather predictions. *Space Weather*. 2017, vol. 15, pp. 418–429. DOI: 10.1002/2016SW001593.

Buresova D., Lastovicka J. Changes in the F1 region electron density during geomagnetic storms at low solar activity. *J. Atmos. Solar-Terr. Phys*. 2001, vol. 63, pp. 537–544. DOI: 10.1016/S1364-6826(00)00167-X.

Kushnarenko G.P., Yakovleva O.E., Kuznetsova G.M. Electron density in the F1-layer over Norilsk in 2007–2014. *Solar-Terr. Phys*. 2019, vol. 5, no. 2, pp. 109–112. DOI: 10.12737/stp-52201915.

Panasyuk M.I., Kuznetsov S.N., Lazutin L.L., Alexeev I.I., Antonova A.E., Belenkaya E.S., Bobrovnikov S.Yu., Veselovsky I.S., et al. Magnetic storms in October 2003.. *Cosmic Res*. 2004, vol. 42, no. 5, pp. 489–534. DOI: 10.1023/B:COSM.0000046230.62353.61.

Picone J.M., Hedin A.E., Drob D.P., Aikin A.C. (GTD7-2000) NRLMSISE-00 Empirical model of the atmosphere: statistical comparisons and scientific issues. *J. Geophys. Res.* 2002, vol. 107, no. A12, p. 1469. DOI: 10.1029/2002JA009430.

Shchepkin L.A., Kuznetsova G.M., Kushnarenko G.P., Ratovsky K.G. Approximation of electron density measurements data in middle ionosphere during the low solar activity. *Solnechno-zemnaya fizika* [Solar-Terr. Phys.]. 2008, vol. 11, pp. 66–69. (In Russian).

Tobiska W.K., Eparvier F.G. EUV97: Improvements to EUV irradiance modeling in the soft X-rays and EUV. *Solar Phys*. 1998, vol. 147, no. 1, pp. 147–159. DOI: 10.1023/A:1004931416167.

Yakovleva O.E., Kushnarenko G.P., Kuznetsova G.M. The atmosphere below 200 km over Norilsk at solar minimum and maximum. *Solar-Terr. Phys*. 2020, vol. 6, no. 3, pp. 86–89. DOI: 10.12737/stp-63202012.

URL: http//ckp-rf.ru/ckp/3056 (accessed March 31, 2021).

URL: http//wdc.kugi.kyoto-u.ac.jp (accessed March 31, 2021).

How to cite this article

Yakovleva O.E., Kushnarenko G.P., Kuznetsova G.M. Behavior of electron density in the ionosphere over Norilsk during the period of decline in solar activity. *Solar-Terrestrial Physics*. 2021. Vol. 7. Iss. 2. P. 70–73. DOI: 10.12737/stp-72202107.